KGF-2 ameliorates acute lung injury via inhibiting TH17 cells-NF-κB-dependent inflammation and activating the PI3K/Akt survival signaling pathway in mice

Linlin Wang[1,*], Jian Wang[1,*], Shimeng Ji[1], Dongni Hou[1], Cuicui Chen[1], Chunxue Bai[1], Jian Zhou[1] and Yuanlin Song[1,2,3]

[1]Department of Pulmonary Medicine, Zhongshan Hospital, Fudan University, Shanghai 200032, China

[2]Shanghai Public Health Clinical Center, Shanghai 201508, China

[3]Zhongshan Hospital, Qingpu Branch, Fudan University, Shanghai 201700, China

[*]Co-author

Correspondence to: *Yuanlin Song,* ***email:*** *song.yuanlin@zs-hospital.sh.cn*
Jian Zhou, ***email:*** *zhou.jian@fudan.edu.cn*
Chunxue Bai, ***email:*** *bai.chunxue@zs-hospital.sh.cn*

Keywords: *LPS induced ALI; Th17 and Treg cells; KGF-2; PI3K/Akt; NF-κB*

Received: *October 20, 2017* ***Accepted:*** *January 03, 2018* ***Published:*** *January 13, 2018*

ABSTRACT

Acute lung injury is characterized by alveolar injury, inflammation, and infiltration of inflammatory cells. Although the protective effects of keratinocyte growth factor-2 on ALI have been defined, the mechanisms remain unclear. Lipopolysaccharides (*Pseudomonas aeruginosa*) was administered intratracheally into mice lungs, and peak lung injury occurred on day 6 after the LPS challenge, with resolution on day 10. A progressive influx of $CD4^+CD25^+Foxp3^+$T cells into the lungs and spleen on day 1, which peaked on day 6, and was maintained at high level on day 10. The percentage of Th17 cells in lung tissue and blood was higher in the ALI group than in the control group, which peaked on day 2, and returned to nearly normal on day 10. KGF-2 attenuated lung injury by inhibiting the prevalence of Th17 cells through STAT3 dysfunction and NF-κB signal, and improved survival rate by activating the PI3K/Akt signal. These results illustrated a new mechanism of KGF-2 on ALI by inhibiting Th17 cells mediated by STAT3-NF-κB, and activating the PI3k/Akt signal.

INTRODUCTION

Acute lung injury (ALI) is the mild form of acute respiratory distress syndrome (ARDS), characterized by damage of the alveolar epithelium and endothelium with accumulation of plasma proteins and flooding in the alveoli causing refractory hypoxemic respiratory failure, inflammatory cells infiltration, and release of pro-inflammatory cytokines [1–2]. ALI can result in refractory hypoxemic respiratory failure and dependence on mechanical ventilation, increasing susceptibility to multiorgan dysfunction and mortality. However, current management is mainly supportive such as mechanical ventilation, but mortality still remains high at about 30–40% [3]. Thus, specific therapies are the need of the hour.

Keratinocyte growth factor-2 (KGF-2) is a member of the fibroblast growth factor family, namely fibroblast growth factor-10. KGF-2 is mainly expressed and secreted by stromal cells and has a high affinity to fibroblast growth factor receptor 2-IIIb, which is mainly expressed on the epithelium; it has a comparatively weaker affinity for fibroblast growth factor receptor 1-IIIb expressed by epithelial and endothelial cells [4–7]. KGF-2 has been found to play an essential role in epithelial-mesenchymal interactions for the proper development of organs such as the lungs [5]. KGF-2 also regulates cell differentiation and migration [8].

The role KGF-2 in ALI has been extensively studied since the 1990s. Those including our previous studies indicated that KGF-2 has protective effects on ALI. Treatment with KGF-2 attenuated severe pulmonary edema and lung injury induced by ischemia/reperfusion [9], ventilator [10], and lipopolysaccharides (LPS) [11], also improved bleomycin-induced pulmonary fibrosis [12], high-altitude pulmonary edema [13]. We also found that concurrent administration of KGF-2 facilitated the clearance of *Pseudomonas aeruginosa* from the lungs, attenuated *P. aeruginosa*-induced lung injury, and extended the 7-day survival rate [14]. However, whether KGF-2 has an influence on the immune responses of ALI and the potential mechanism still remain unclear.

T- and B-lymphocytes are major cells of the adaptive immune system and can manage the immune response by directing other cells to perform cytotoxic and phagocytic functions. Regulatory T ($CD4^+CD25^+Foxp3^+$Tregs) and T helper (Th)-17 cells, which are the subsets of $CD4^+$T cells, have become an active topic of research in the pathogenesis or resolution of ALI/ARDS. $CD4^+C25^+Foxp3^+$Tregs play important roles in suppressing the inflammatory response mainly by releasing anti-inflammatory cytokines such as IL-10 and TGF-β or contact-dependent suppression [15]. $CD4^+C25^+Foxp3^+$Tregs contribute to the resolution of ALI by modifying the innate immune response [16] and decreasing fibrocyte recruitment [17]. An increased alveolar $CD4^+C25^+Foxp3^+$Tregs ratio in ARDS is associated with increased 30-day mortality [18]. Th17 cells play potent pro-inflammatory roles by secreting cytokine IL-17A, IL-22, IL-6, and TNF-α [15, 19]. IL-17 potently induces the production of IL-8 and G-CSF from epithelial cells and fibroblasts, thereby resulting in neutrophil activation and recruitment. Patients with early ARDS appeared to have increased peripheral circulating Th17 cells and their associated cytokines [20]. These studies indicated that $CD4^+C25^+Foxp3^+$Tregs and Th17 cells play important roles in the pathogenesis and resolution of ALI. However, the regulation and mechanisms of KGF-2 on $CD4^+C25^+Foxp3^+$Tregs and Th17 cells are yet ill defined.

In the current study, we examined parameters related to $CD4^+C25^+Foxp3^+$Tregs and Th17 cells in the pathogenesis and resolution of ALI. Additionally, we investigated whether KGF-2 regulated $CD4^+C25^+Foxp3^+$Tregs and Th17 cells, and dissected the mechanisms involving certain signaling pathways.

RESULTS

Measurement of lung injury

Measures of lung injury include lung histology, lung vascular permeability (W/D weight ratio and BAL protein), and total cell and differential counts. Lung histology revealed a marked increase of inflammatory cells including neutrophils, macrophages, and lymphocytes by day 1 after intrathecal LPS injection (Figure 1B), with increased interstitial thickening and inflammatory cells on day 2 (Figure 1C), and peaking on day 6 (Figure 1D). By day 10, the lung injury was obviously alleviated and histologic changes were similar to those seen at days 1 and 10 (Figure 1B and 1E).

The W/D weight ratio of the lung and protein concentration in BALF are markers of vascular permeability. Both parameters showed increased lung vascular permeability on day 1 which persisted on day 6, but was markedly reduced on day 10. In order to assess the effect of LPS on inflammation, total and differential white blood cell counts in BALF were also analyzed. The total cell numbers in BALF significantly increased on day 1, and peaked two days later, and returned to nearly normal by day 10. Approximately 60–80% of the neutrophils were maintained from day 1 to day 2. The absolute value of neutrophils was at the highest level on day 2. The trend was similar for total cell number in BALF. The percentage of macrophages significantly decreased after LPS injection compared to the control group, was maintained at about 10% from day 1 to day 6, and showed marked elevation on day 10. The absolute value of macrophages showed no obvious change in either group (Figure 1G).

The inflammatory mediators significantly increased on day 1 and decreased to nearly normal on day 10. However, different cytokines had their own features. IL-1β in BALF and plasma peaked on day 2, IL-6 in BALF and plasma peaked on day 1, and TNF-α in BALF and plasma were similar between day 1 and day 2 (Figure 1H).

$CD4^+C25^+Foxp3^+$Tregs and Th17 cells evaluated in LPS-induced acute lung injury

Studies reported the important roles of $CD4^+C25^+Foxp3^+$Tregs in the inhibition of inflammation and resolution of lung injury. Thus, we hypothesized that $CD4^+C25^+Foxp3^+$Tregs play critical roles in the pathogenesis and resolution of lung injury. Thus, to understand the potential contribution of specific lymphocyte subsets to LPS, we evaluated $CD4^+CD25^+Foxp3^+$Tregs on lung and spleen by flow cytometry. We observed a progressive influx of $CD4^+CD25^+Foxp3^+$Tregs into lung and spleen on day 1, which peaked on day 6 and was maintained at a high level on day 10 (Figure 2A and 2B). $CD4^+CD25^+Foxp3^+$Tregs related cytokines IL-10 and TGF-β in BALF and plasma had similar change trend with the percentage of $CD4^+CD25^+Foxp3^+$Tregs (Figure 2E).

IL-17A and IL-22 are the main cytokines released by Th17 cells. We measured the levels of these two cytokines in BALF and plasma. As expected, IL-17 and IL-22 in the ALI group increased significantly after LPS injection and peaked at day 2 (Figure 2E). To further confirm the effect of LPS on Th17 cells expansion, lung tissues and blood were collected for flow cytometry analysis. Because PMA

stimulation can downregulate CD4, we gated $CD3^+CD8^-$ T cells to determine as $CD4^+$T cells. As shown in Figure 2C and 2D, the percentage of Th17 cells in lung tissues and blood was higher in ALI group than in control group, peaked at D2, and returned to nearly normal on day 10.

KGF-2 exerted protective effects on LPS-induced ALI

First, we detected the influence of ALI induced by LPS on KGF-2 expression. As shown in Figure 3A,

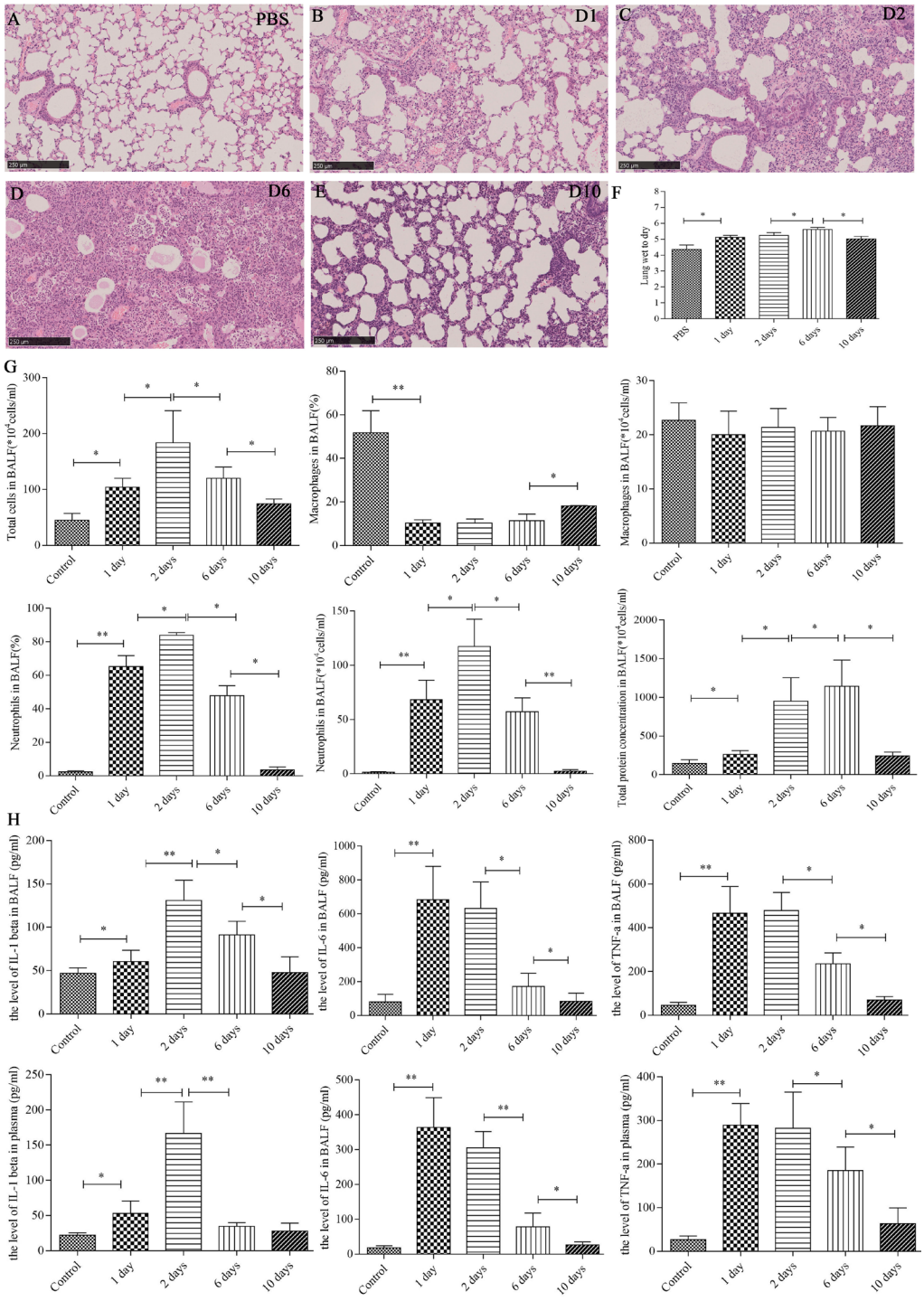

Figure 1: Measurement of lung injury at different time points. Mice (n = 5 per group per time point) were challenged with intrathecal LPS. **(A-E)** Lung sections were stained with H&E (magnification, 40×). **(F)** Lung W/D was measured. **(G)** Total cell counts, differential cell counts, and BALF total protein were determined in mice after treatment with PBS or LPS. **(H)** BALF and plasma cytokines including IL-1β, IL-6, and TNF-α were assessed at different time points.

lung KGF-2 mRNA level in ALI group was significantly lower than that in PBS group. Moreover, our previous studies indicated that KGF-2 had the potential to protect against ALI. To further investigate the roles of KGF-2, we instilled KGF-2 into the trachea to evaluate its effects on LPS-induced ALI. The survival rate in the KGF-2 group was significantly higher at 45% than 10% in LPS group (Figure 3B). Mice treated with KGF-2 lose less weight and recover faster than those in LPS group (Figure 3C). Studies indicated that PI3K/Akt is the survival signaling pathway involved. To evaluate whether the PI3K/Akt signaling pathway involved in the KGF-2 protective effects on ALI, we detected the level of Akt phosphorylation. We found that the level of Akt phosphorylation in mice with ALI treated with KGF-2 was obviously upregulated (Figure 3D). Histological features of LPS-induced ALI, including protein-rich edema fluid in the alveolar space, leukocyte accumulation, hemorrhage and bronchial wall thickening with inflammatory cells, were improved by KGF-2 treatment, and lung injury score was significantly lower than that in control mice receiving no treatment; the lung W/D ratio was markedly reduced (Figure 3E). Total cells (Figure 4A), protein concentration (Figure 4B), absolute counts and proportion of neutrophils (Figure 4D) decreased while macrophages increased in BALF (Figure 4C). Moreover, the inflammatory mediators in BALF and

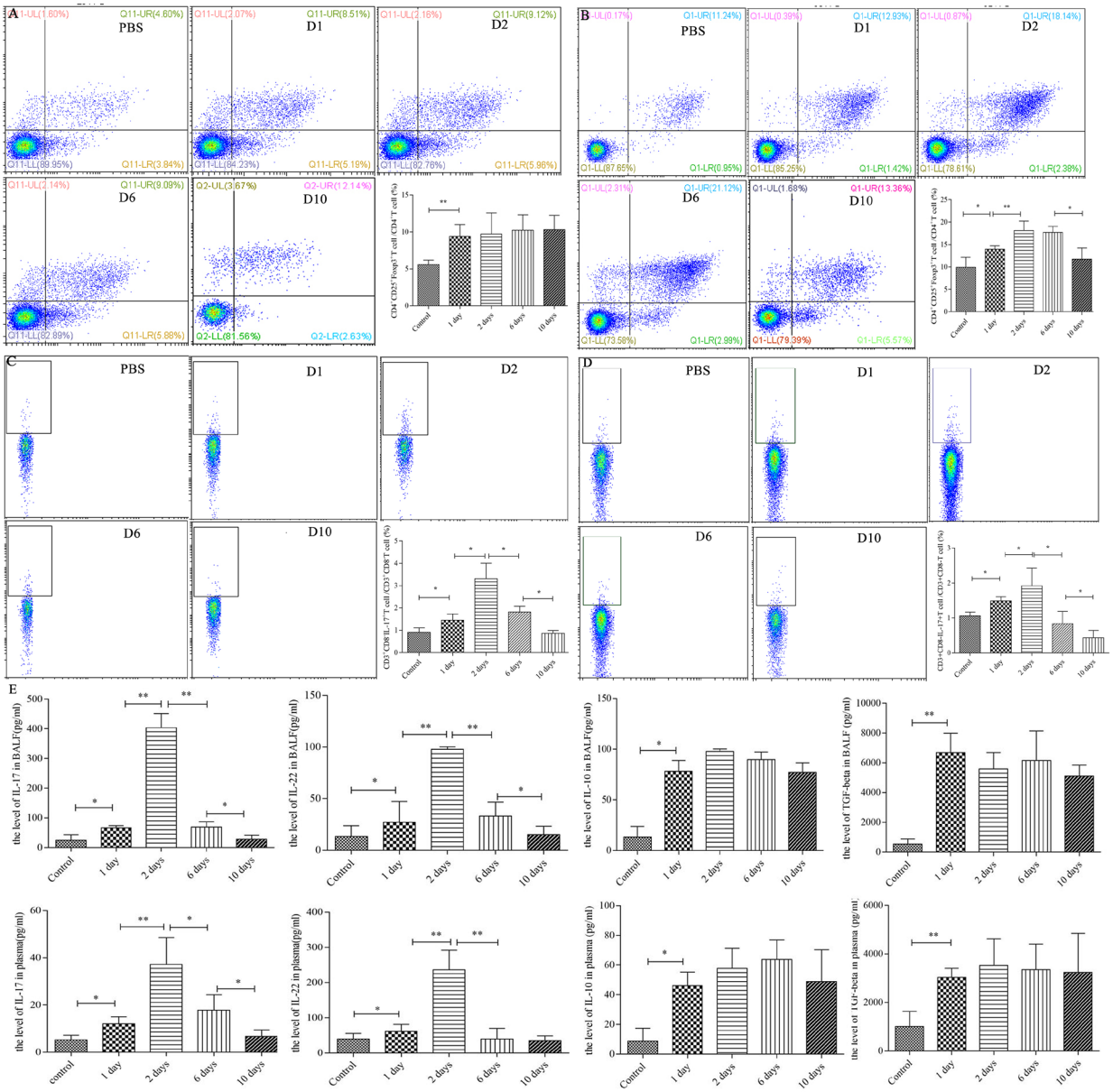

Figure 2: CD4$^+$CD25$^+$Foxp3$^+$Tregs and CD3$^+$CD8-IL-17$^+$Th17 cells increase after lung injury with intrathecal LPS. (A and B) CD4$^+$CD25$^+$Foxp3$^+$Tregs from lung and spleen were analyzed by flow cytometry. **(C and D)** CD3$^+$CD8-IL-17$^+$Th17 cells from lung and blood were assessed by flow cytometry. **(E)** BALF and plasma cytokines including IL-17, IL-22, IL-10, and TGF-β were assessed at different time points.

plasma including IL-1β (Figure 4E), IL-6 (Figure 4F) and TNF-α (Figure 4G), were markedly reduced.

KGF-2 downregulated Th17 cells and $CD4^+CD25^+Foxp3^+$Tregs by decreasing STAT3 and STAT5 phosphorylation

Studies showed that KGF-2 could downregulate IL-6 levels, which is an important cytokine to induce the proliferation and differentiation of Th17 cells in LPS-induced ALI. Thus, we determined the effect of KGF-2 on Th17 cells. KGF-2 significantly decreased the percentage of Th17 cells (Figure 5B and 5C). Moreover, we found that KGF-2 also significantly downregulated $CD4^+CD25^+Foxp3^+$Tregs (Figure 5A).

Signal transduction and transcription activation factors (STATs) are a group of intracellular transcription factors and play important roles during the differentiation of T cells. STAT3 is a positive regulatory element for Th17 polarization. Thus, we investigated the level of STAT3 in the lung, and found that pSTAT3 significantly reduced after KGF-2 treatment (Figure 5D). STAT5 is responsible

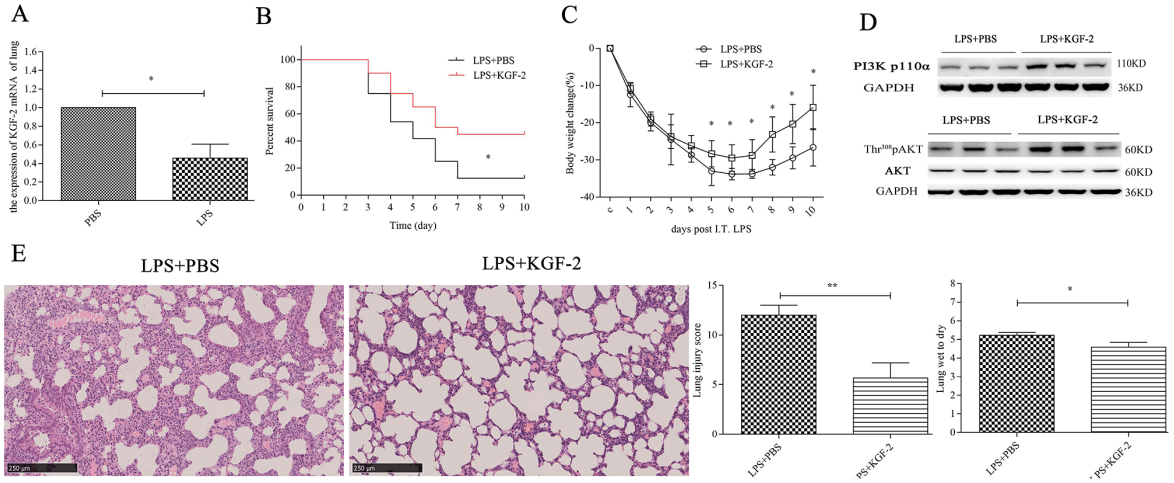

Figure 3: The protective effects of KGF-2 on LPS-induced ALI. (A) KGF-2 mRNA expression in the lung**. (B)** Survival rates of mice in control and KGF-2 groups. The 10-day survival rate was calculated and plotted following LPS-induced ALI in control and KGF-2 groups (n = 20 mice per group). **(C)** Body weight changes in the LPS-challenged mice treated with or without KGF-2. **(D)** Western blot analysis detected the protein level of PI3K 110α and phosphorylation of AKT. **(E)** Lung sections were stained with H&E to evaluate lung injury (magnification, 40×). Lung W/D was measured.

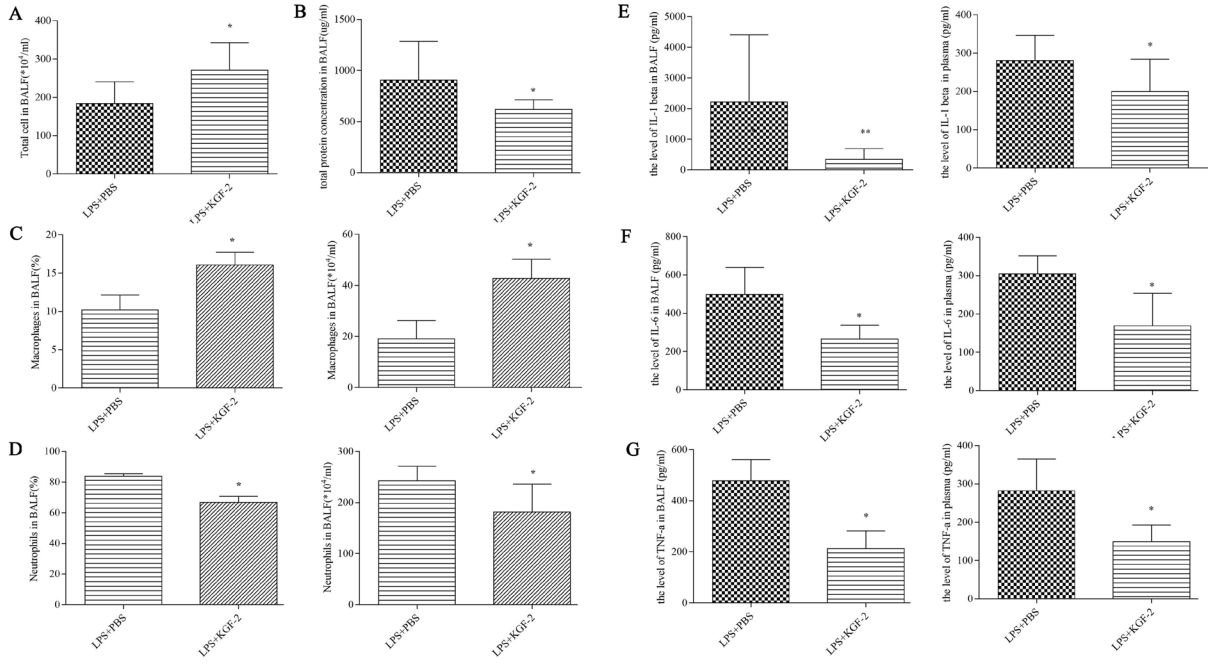

Figure 4: Total cells **(A)**, total protein concentration **(B),** and percentage of macrophages and neutrophils **(C and D)** in BALF were tested. The levels of IL-1β **(E)**, IL-6 **(F)**, and TNF-α **(G)** in BALF and plasma were assessed.

for $CD4^+CD25^+Foxp3^+$Tregs differentiation and also is negative regulation of Th17 cell differentiation. We found that KGF-2 treatment significantly reduced STAT5 phosphorylation (Figure 5D).

Moreover, we found that KGF-2 also decreased the Th17 cells relative to cytokines IL-17 and IL-22 levels in BALF and plasma, and upregulated the levels of IL-10 and TGF-β secreted mainly by Treg cells in BALF and plasma (Figure 5E).

KGF-2 inhibited NF-κB signaling pathway to decrease Th17 cells and $CD4^+CD25^+Foxp3^+$Tregs

As NF-κB signaling pathway is the major inflammatory mediator, we further studied the effects of KGF-2 treatment on NF-κB signaling activation in LPS-induced ALI. The proportion of phosphorylated NF-κB p65 in total NF-κB p65 was reduced after KGF-2 treatment (Figure 6A). TLR-4 expression level in lung also has been detected. We found that TLR-4 significantly increased in LPS-induced ALI, and was reduced after KGF-2 treatment (Figure 6B). To further investigate the mechanism of KGF-2 on Th17 cells, we intraperitoneally injected the inhibitor of NF-κB BAY11-7082 to LPS-induced ALI mice and found that the percentage of Th17 cells and $CD4^+CD25^+Foxp3^+$Tregs obviously downregulated (Figure 6C and 6D).

DISCUSSION

There is accumulating evidence indicating that Th17 cells and $CD4^+CD25^+Foxp3^+$Tregs that belong to

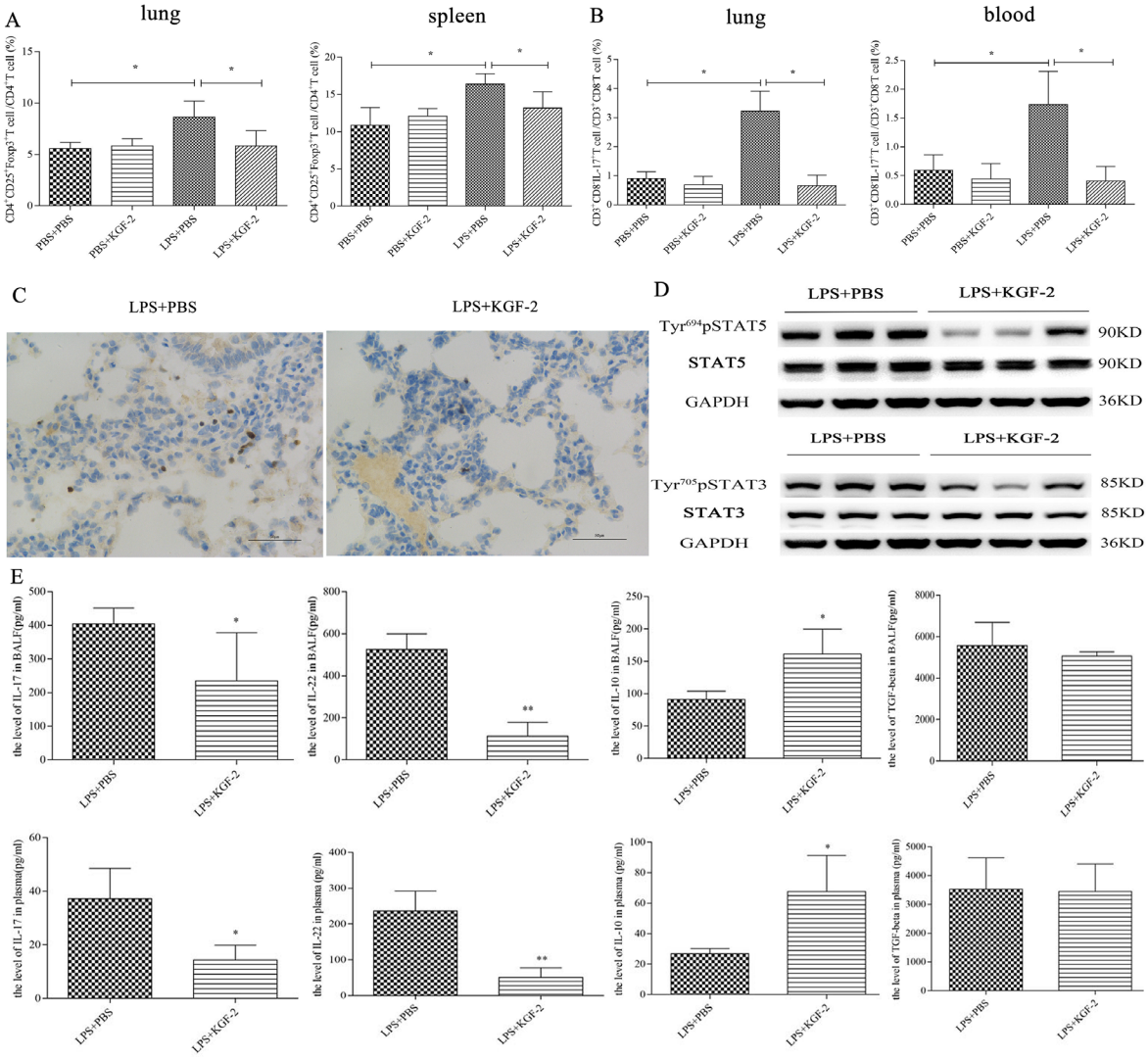

Figure 5: KGF-2 downregulated Th17 and Treg cells by regulating pSTAT3 and pSTAT5. (A) $CD4^+CD25^+Foxp3^+$Tregs in lung and spleen from the ALI model treated with or without KGF-2. **(B)** $CD3^+CD8$-IL-17^+Th17 cells of lung and blood were also evaluated in the ALI model treated with or without KGF-2. **(C)** ROR-γt was detected by immunohistochemistry (IHC:400). **(D)** The protein level of phosphorylated and total STAT3 and STAT5. **(E)** The levels of IL-17, IL-22, IL-10, and TGF-β in BALF and plasma were assessed.

$CD4^+$T cells play important roles in the pathogenesis and resolution of ALI/ARDS. A series of studies including our previous studies have shown that KGF-2 has potential protective effects in ALI induced by various stresses. However, the mechanisms remain incompletely understood. The present study investigated the role of KGF-2 on Th17 and the signaling pathways of KGF-2 regulating Th17 cells and $CD4^+CD25^+Foxp3^+$Tregs. In this report, we found that KGF-2 attenuated lung injury by inhibiting Th17 cells-NF-κB signaling pathway, and activating the PI3K/Akt signal (Figure 7).

$CD4^+CD25^+Foxp3^+$Tregs is essential for maintaining immune homeostasis and can reduce inflammation and tissue damage. $CD4^+CD25^+Foxp3^+$Tregs could be activated during ALI development, and the increase of $CD4^+CD25^+Foxp3^+$Tregs even became a risk factor for predicting poor outcome of ARDS patients [18, 20]. The depletion of $CD4^+CD25^+Foxp3^+$Tregs resulted in a more severe course of LPS-induced ALI, indicating that $CD4^+CD25^+Foxp3^+$Tregs contribute to a positive outcome [16]. In the present study, we found that the percentage of $CD4^+CD25^+Foxp3^+$Tregs increased synchronously with hyper-inflammatory early stage of ALI. We speculated that the prevalence of $CD4^+CD25^+Foxp3^+$Tregs in ALI is primarily to provide negative feedback. Therefore, the percentage of $CD4^+CD25^+Foxp3^+$Tregs decreased when the treatment of KGF-2 alleviated the inflammation of LPS-induced ALI and downregulated the prevalence of Th17 cell.

Th17 cells play important roles in autoimmune inflammatory diseases and infectious diseases, and mediated acute inflammatory responses. In ALI, Th17 cells and IL-17A is increased at an early phase, induces inflammatory cytokines, and affects neutrophil kinetics [21, 22]. In our study, Th17 cells in lung and peripheral blood were also increased in the early stage of ALI induced by LPS. We also found that the change in IL-17A was consistent with the change of Th17 cells, neutrophils, and related lung injury parameters. The differentiation and proliferation of Th17 cells are determined by the microenvironment. TGF-β and IL-6 are the main cytokines to induce the differentiation of Th17 cells [23]. High level TGF-β induces the differentiation of $CD4^+CD25^+Foxp3^+$Tregs, but in the IL-6-rich inflammation milieu, the generation of Th17 cells is enhanced. In this report, both TGF-β and IL-6 were increased in serum and BALF of mice with ALI. Thus, we thought that the induced Th17 cells from naïve CD4+T cells maybe the main source of the increased Th17 cells in mice with ALI.

PI3K/Akt signaling pathways are important pathways involved in the proliferation and differentiation of some cells, and is a critical growth and survival pathway in many biological processes [24]. Akt has been implicated in protection against lung injury [25], and KGF-2 activates the PI3K signaling pathway [26, 27]. Our previous studies have found that KGF-2

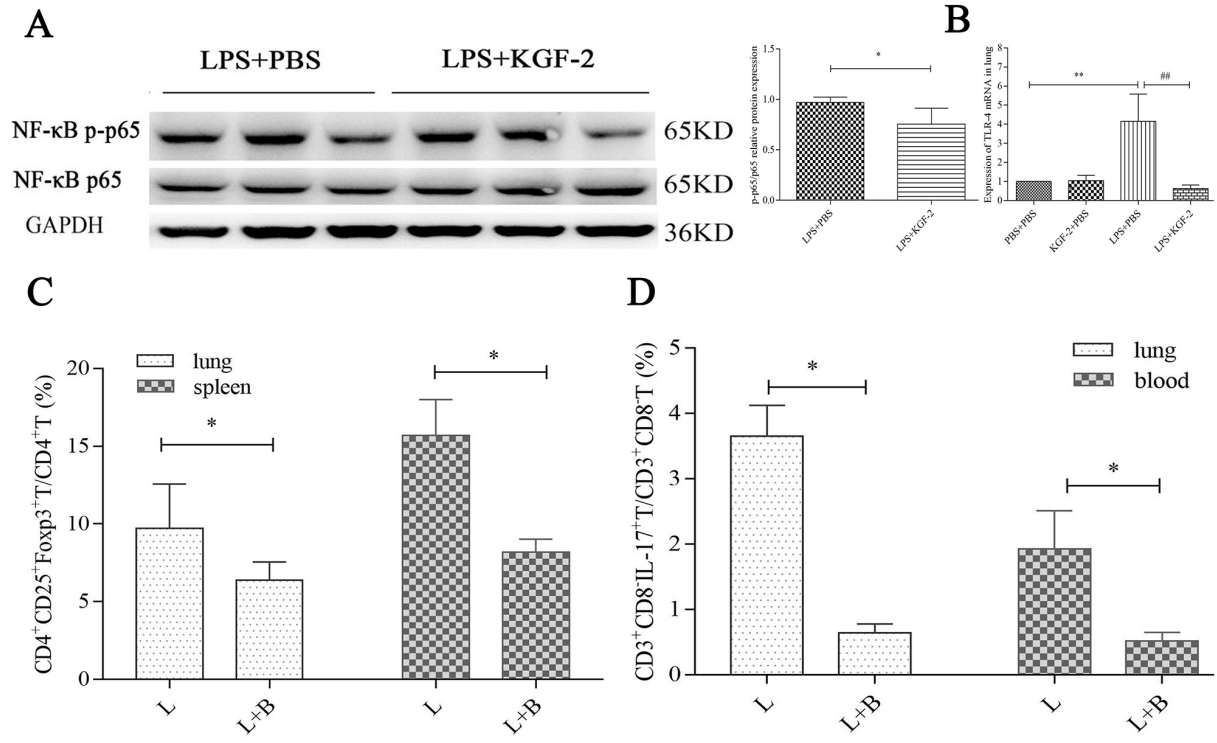

Figure 6: KGF-2 inhibited the proliferation of Treg and Th17 cells through downregulation of NF-κB p65 phosphorylation. (A) The phosphorylation of NF-κB p65 was evaluated by WB. **(B)** TLR-4 mRNA was measured by RT-PCR. **(C)** $CD4^+CD25^+Foxp3^+$Tregs in the lung and spleen of the ALI model treated with or without NF-κB inhibitor. **(D)** $CD3^+CD8^-IL\text{-}17^+$Th17 cells of the lung and blood were also evaluated in the ALI model treated with or without NF-κB inhibitor.

instilled intratracheally 72 hours before LPS challenge or mixed with *Pseudomonas aeruginosa* could protect ALI (9-11, 14). Thus, we given the ALI model the KGF-2 mixed with LPS to mock the immediate treatment of KGF-2 after the attach of ALI in the present study. We found that injection of KGF-2 mixed with LPS could improve the survival rate and weight of mice with ALI. To evaluate whether the PI3K/Akt signaling pathway is involved in the KGF-2 protective effects on ALI, we detected the level of Akt phosphorylation. We found that the level of Akt phosphorylation in mice with ALI treated with KGF-2 was markedly upregulated.

Phosphorylated STAT3 can provide a rapid membrane for the nucleus mechanism regulating the expression of nuclear translation factor, and promote the expansion of Th17 cells [28, 29]. STAT5 is responsible for the differentiation of $CD4^+CD25^+Foxp3^+$Tregs [30]. Our study found that KGF-2 downregulated the prevalence of Th17 and $CD4^+CD25^+Foxp3^+$Tregs, and decreased the levels of STAT3 and STAT5 phosphorylation. To further evaluate the possible mechanism of KGF-2 regulating Th17 and $CD4^+CD25^+Foxp3^+$Tregs, we intraperitoneally administered the NF-κB inhibitor (BAY11-7082) to mice with ALI, and found that the proportion of Th17 and $CD4^+CD25^+Foxp3^+$Tregs were downregulated after the inhibition of NF-κB signaling pathway. A large number of studies have shown that Akt activation positively controls NF-κB-dependent transcription, and blocking PI3K/Akt signaling leads to a marked reduction of NF-κB activity [31]. In our study, we found that KGF-2 activates the PI3K/Akt signaling pathway, which seemed to result in enhanced NF-κB activity in ALI. Nevertheless, we found that KGF-2 inhibited NF-κB activity in our experiments. The above data clearly show that the inhibitory effect of KGF-2 on NF-κB activity is not mediated by PI3K/Akt signaling pathway. However, we are still unsure of the mechanism of action of KGF-2 modulation of NF-κB.

Although our study highlighted the mechanism of KGF-2 to protect ALI model *in vivo*, it did not evaluate the role of KGF-2 on the differentiation and proliferation of Th17 cells and $CD4^+CD25^+Foxp3^+$Tregs *in vitro*. And it did not address the mechanism of KGF-2 modulating NF-κB. In the present study, the total cells in BALF in mice treated with KGF-2 obviously increased, and we found that the increased cells were mainly macrophages. However, the source of macrophages and the possible mechanism remain unknown. Future experiments will seek to clarify these issues.

In conclusion, we demonstrate that KGF-2 can protect the ALI murine model via inhibiting Th17 cells-NF-κB-dependent inflammation and activating the PI3K/Akt survival signaling pathway. These findings have implications for understanding the pathophysiology of ALI induced by LPS and the mechanisms of KGF-2 to protect ALI, provide new insights to treat ALI/ARDS through immune system regulation.

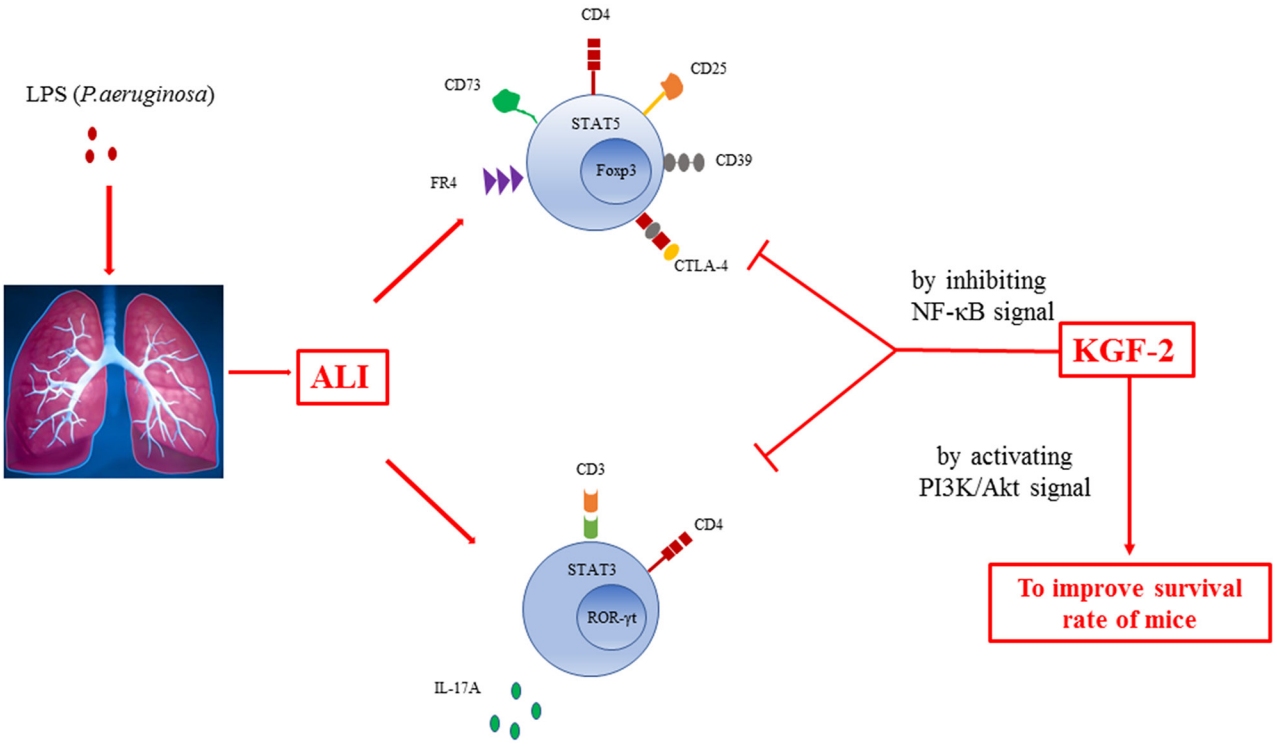

Figure 7: A proposed framework for KGF-2 against LPS (*P. aeruginosa*)-induced ALI by inhibiting NF-κB signal and activating the PI3K/Akt survival signal pathway.

MATERIALS AND METHODS

Animals and experimental protocols

Male C57BL/6 mice aged 8–10 weeks and weighed 20–25 g were used and bred carefully in the Medicine School of Fudan University in accordance with ethical guidelines of the National Institutes of Health on Animal Care. Mice were raised in specific pathogen-free cages and maintained at temperatures between 20 and 25°C and relative humidity of 50–70%. The experimental protocols were approved by the Animal Care and Use Committee, Fudan University, Shanghai.

Mice were anesthetized with an intraperitoneal injection of 25 mg/kg Avertin (Sigma-Aldrich, St Louis, MO, USA) and intratracheally injected with either 5 mg/kg LPS (*Pseudomonas aeruginosa* 10, Sigma-Aldrich, St Louis, MO, USA) dissolved in PBS or an equal volume of vehicle (PBS only). To investigate the role of KGF-2 (recombinant human KGF-2, recombinant product from *E. coli* after purification; MW 19.3 kDa; Newsummit Pharmaceutical Company, Shanghai, China) in lung injury induced by LPS, KGF-2 (5 mg/kg) mixed with LPS or PBS, was intratracheally injected. To clarify the role of NF-κB pathway, 20 μg/kg BAY 11-7082 (Sigma-Aldrich, St Louis, MO, USA), the inhibitor of IκBα phosphorylation, was injected intraperitoneally 30 min prior to LPS administration.

Mice were euthanized 1, 2, 6, and 10 days after LPS administration or 2 days after KGF-2 treatment. All mice were anesthetized intraperitoneally with chloral hydrate. Blood samples were collected by removing the eyeball. The lung lobes were prepared for histological examination, wet-to-dry (W/D) weight ratio, lung single cell for flowcytometry, western blotting, and RT-PCR. Bronchoalveolar lavage fluid (BALF) also was collected.

Analysis of BALF

BALF was centrifuged at 1500 *g* for 10 min at 4°C, and the supernatant was stored at −80°C until further analysis, while the cell pellet was used for the cell count. The total number of nucleated cells in BALF was counted with a hemocytometer. The resuspended BALF cells were centrifuged, transferred to slides, and stained with Wright–Giemsa stain. Neutrophils and macrophages on all slides were quantified by counting a total of 200 cells/slide at 40× magnification.

Lung vascular permeability

The right lower lobe of the lung was used to calculate the lung W/D weight ratio. The weight was immediately checked after isolation and after being oven dried at 60°C for 72 h. The wet weight was divided by the dried weight to obtain the W/D ratio. Total protein concentration in BALF was measured by) (Enhanced BCA Protein Assay Kitenhanced BCA protein assay kit according to the manufacturer's instruction (Biyuntian, Shanhgai, China).

Cytokines assay

The concentrations of IL-1β, IL-6, TNF-a, IL-17, IL-22, IL-10, and TGF-β in serum and BALF supernatant were determined by enzyme-linked immunosorbent assay (ebioscience, San Diego, CA, USA). All procedures followed the manufacturer's instructions.

Lung histopathology

The right upper lobe of the lung was analyzed by histology. The lung was fixed in 10% formalin, dehydrated, embedded in paraffin, sectioned, and stained with hematoxylin/eosin (HE), and the morphological lesions and changes in lung tissue were observed under a light microscope. The histological score of lung injury including the summed scores of atelectasis, alveolar and interstitial edema, pulmonary hemorrhage, and interstitial infiltration of inflammatory cells, and was scored by a pathologist blinded to the sample.

Quantitative real-time polymerase chain reaction

Total RNA was extracted using the TRIzol reagent (Invitrogen, CA, USA). RNA was reverse-transcribed into cDNA using the cDNA kit (TOYOBO, Japan). The primers were designed and synthesized by Shenggong (Shanghai, China). For amplification, the SYBR-Green I Real-Time PCR kit (TOYOBO) was used. Each reaction was run in triplicate and normalized to the housekeeping gene β-actin transcripts.

Preparation of lung single cell

Mouse lungs were dissected into single lobes and rinsed in a petri dish containing PBS to remove the thymus, heart, trachea, connective tissue, and efferent and afferent blood vessels. The lobes were transferred into gentleMACS C tube containing the enzyme mix (buffer S, enzyme D, and enzyme A) (Miltenyi, Bergisch Gladbach, Germany), and run on the gentleMACS program m-lung-01. The samples were then incubated for 30 min at 37°C, and run on the gentleMACS program m-lung-02. Finally, the sample was centrifuged to collect the single cells.

Flow cytometry

Expression markers on the surface of T cells were determined by fluorescence-activated cell sorting analysis, following surface staining or intracellular staining with specific anti-mouse antibodies. Cells were incubated with Fc Block-2.4G2 (BD Biosciences PharMingen, San Diego,

CA, USA) antibody to block Fcγ III/II receptors before staining with a specific antibody. The following antibodies (ebioscience) were used for surface staining: FITC-conjugated anti-CD3, FITC-conjugated anti-CD4, PE-cy7-conjugated anti-CD8, PE-cy7-conjugated anti-CD25, PE-conjugated anti-Foxp3, PE-conjugated anti-IL-17A, APC-conjugated anti-F4/80, PE-conjugated anti-Gr-1, FITC-conjugated anti-CD11b, and PE-conjugated isotype.

For the analysis of $CD4^+CD25^+Foxp3^+$Tregs, the prepared lung single cells and splenocytes were collected into tubes without stimulation of phorbol 12-myristate 13-acetate (PMA), ionomycin, and brefeldin A (BD Biosciences). The RBCs were lysed using cell lysing solution (BD Biosciences). Cells were incubated with surface markers anti-mouse CD4-FITC and anti-mouse CD25-PE-cy7 antibodies, followed by fixation and permeabilization with Foxp3 staining buffer (ebioscience) and intracellular staining with anti-mouse Foxp3-PE antibody. To detect the phenotypes of Th17 cells in whole blood and lung, the mixture of PMA, ionomycin, and brefeldin A was used to stimulate cytokine expression of Th17 cells for 6 h. The surface markers of anti-mouse CD3-FITC and CD8-PE-cy7 were used to determine $CD4^+$T cells ($CD3^+CD8^-$T cells), as CD4 is downregulated when stimulated by PMA. The cells were stained with CD3-FITC and CD8-PE-cy7 antibodies, and then fixed and permeabilized using Fix/Perm Reagent (BD Biosciences), followed by intracellular staining with IL-17A-PE antibody. Isotype controls of IL-17A and Foxp3 were used to correct the compensation and confirm antibody specificity. For the analysis of neutrophils and macrophages, the cells in BALF were stained with F4/80-APC, Gr-1-PE, and CD11b-FITC antibodies.

After all procedures, the stained cells were analyzed by flow cytometry (Beckman CytoFLEX). Lymphocytes were gated with characteristic low forward scatter/side scatter, and CytExpert 2.0 (Beckman) software were used to analyze the data.

Western blot analysis

The protein levels of relative genes were analyzed with western blot. Total protein and phosphorylated protein were extracted. Briefly, lung tissues were lysed and homogenized with RIPA (Radio Immunoprecipitation AssayRadio Immunoprecipitation AssayRadio Immunoprecipitation Assay) buffer supplemented with phosphatase inhibitors and/or protease. After being mixed and incubated on ice for four times every 15 min, the homogenate was centrifuged at 12000 ×*g* for 15 min at 4°C. A BCA kit was used to determine the concentration of supernatant. An equal amount of protein was separated through electrophoresis on SDS-PAGE and then transferred to polyvinylidene fluoride membranes. After blocking for 1 h, the membrane was incubated with antibodies overnight at 4°C. The membrane was washed 3 times with PBST, and then the second antibody was incubated at 37°C for 1 h. Protein bands were exposed with enhanced ECL kits and analyzed with Quantity One software (Bio-Rad).

For western blot analysis, the following primary antibodies purchased from CST (Cell Signaling Technology, Danvers, MA, USA) were used: anti-pSTAT5 Tyr694 (1:1000), anti-pSTAT3 Tyr705 (1:1000), anti-PI3K 110α (1: 1:1000), anti-pAKT Thr308 (1: 1:1000), and GAPDH (1: 1:1000).

Immunohistochemistry

Immunohistochemistry was used to analyze the protein levels of ROR-γt in lung tissues. Briefly, lung sections were embedded in paraffin and sectioned to 5-μm thickness, followed by dewaxing in xylene and rehydration. Endogenous peroxidases were inhibited with 0.5% hydrogen peroxide in methanol for 10 min, and slides were incubated overnight at 4°C with a rabbit monoclonal IgG antibody against ROR-γt (Abcam, Cambridge, MA). After washing, sections were covered with DAB and hematoxylin.

Statistics

SPSS17.0 statistical software for Windows was applied for all statistical analysis. Differences between groups were examined for statistical significance by Kruskal–Wallis *H* test. Data are expressed as mean ± standard deviation (SD). $P < 0.05$ was considered statistically significant.

Author contributions

Linlin Wang performed research, participated in the analysis of data and wrote the paper. Jian Wang, Shimeng Ji, Dongni Hou and Cuicui Chen participated in the analysis of data. Yuanlin Song, Jian Zhou and Chunxue Bai participated in the design of the study, helped write the paper and revised the manuscript. All authors read and approved the final manuscript.

CONFLICTS OF INTEREST

The authors have stated explicitly that there are no conflicts of interest in connection with this article.

GRANT SUPPORT

This research was supported by the National Natural Science Foundation of China (81100046, 30930090, 81170056, 81770075, 81630001, 81490533, 81400018, 81570028, 81770039, 81500026), and by grant B115 from Shanghai Leading Academic Discipline Project. Dr. Yuanlin Song was supported by the Program for Professor

of Special Appointment (Eastern Scholar) at Shanghai Institutions of Higher Learning and Key Medical grant from Shanghai Science and Technology Committee (11411951102, 12JC1402300), by the State Key Basic Research Program (973) project (2015CB553404), and by Doctoral Fund of Ministry of Education of China (20130071110044).

REFERENCES

1. Wheeler AP, Bernard GR. Acute lung injury and the acute respiratory distress syndrome: A clinical review. Lancet. 2007; 369:1553–1564.
2. Ware LB, Matthay MA. The Acute respiratory distress syndrome. N Engl J Med. 2000; 342:1334–1349.
3. Sweeney RM, McAuley DF. Acute respiratory distress syndrome. Lancet. 2016; 388:2416–2430.
4. Min H, Danilenko DM, Scully SA, Bolon B, Ring BD, Tarpley JE, DeRose M, Simonet WS. Fgf-10 is required for both limb and lung development and exhibits striking functional similarity to drosophila branchless. Genes Dev. 1998; 12:3156–3161.
5. Ware LB, Matthay MA. Keratinocyte and hepatocyte growth factors in the lung: roles in lung development, inflammation, and repair. Am J Physiol Lung Cell Mol Physiol. 2002; 282:L924–L940.
6. Beer HD, Vindevoghel L, Gait MJ, Revest JM, Duan DR, Mason I, Dickson C, Werner S. Fibroblast growth factor (FGF) receptor 1-IIIb is a naturally occurring functional receptor for FGFs that is preferentially expressed in the skin and the brain. J Biol Chem. 2000; 275:16091–16097.
7. Emoto H, Tagashira S, Mattei MG, Yamasaki M, Hashimoto G, Katsumata T, Negoro T, Nakatsuka M, Birnbaum D, Coulier F, Itoh N. Structure and expression of human fibroblast growth factor-10. J Biol Chem. 1997; 272:23191–23194.
8. Jimenez PA, Rampy MA. Keratinocyte growth factor-2 accelerates wound healing in incisional wounds. J Surg Res. 1999; 81:238–242.
9. Fang X, Wang L, Shi L, Chen C, Wang Q, Bai C, Wang X. Protective effects of keratinocyte growth factor-2 on ischemia-reperfusion-induced lung injury in rats. Am J Respir Cell Mol Biol. 2014; 50:1156–1165.
10. Bi J, Tong L, Zhu X, Yang D, Bai C, Song Y, She J. Keratinocyte growth factor-2 intratracheal instillation significantly attenuates ventilator-induced lung injury in rats. J Cell Mol Med. 2014; 18:1226–1235.
11. Tong L, Bi J, Zhu X, Wang G, Liu J, Rong L, Wang Q, Xu N, Zhong M, Zhu D, Song Y, Bai C. Keratinocyte growth factor-2 is protective in lipopolysaccharide-induced acute lung injury in rats. Respir Physiol Neurobiol. 2014; 201:7–14.
12. Gupte VV, Ramasamy SK, Reddy R, Lee J, Weinreb PH, Violette SM, Guenther A, Warburton D, Driscoll B, Minoo P, Bellusci S. Overexpression of fibroblast growth factor-10 during both inflammatory and fibrotic phases attenuates bleomycin-induced pulmonary fibrosis in mice. Am J Respir Crit Care Med. 2009; 180:424–436.
13. She J, Goolaerts A, Shen J, Bi J, Tong L, Gao L, Song Y, Bai C. KGF-2 targets alveolar epithelia and capillary endothelia to reduce high altitude pulmonary oedema in rats. J Cell Mol Med. 2012; 16:3074–3084.
14. Feng N, Wang Q, Zhou J, Li J, Wen X, Chen S, Zhu Z, Bai C, Song Y, Li H. Keratinocyte growth factor-2 inhibits bacterial infection with pseudomonas aeruginosa pneumonia in a mouse model. J Infect Chemother. 2016; 22:44–52.
15. Noack M, Miossec P. Th17 and regulatory T cell balance in autoimmune and inflammatory diseases. Autoimmun Rev. 2014; 13:668–767.
16. D'Alessio FR, Tsushima K, Aggarwal NR, West EE, Willett MH, Britos MF, Pipeling MR, Brower RG, Tuder RM, McDyer JF, King LS. CD4+CD25+Foxp3+ Tregs resolve experimental lung injury in mice and are present in humans with acute lung injury. J Clin Invest. 2009; 119:2898–2913.
17. Garibaldi BT, D'Alessio FR, Mock JR, Files DC, Chau E, Eto Y, Drummond MB, Aggarwal NR, Sidhaye V, King LS Regulatory T cells reduce acute lung injury fibroproliferation by decreasing fibrocyte recruitment. Am J Respir Cell Mol Biol. 2013; 48:35–43.
18. Adamzik M, Broll J, Steinmann J, Westendorf AM, Rehfeld I, Kreissig C, Peters J. An increased alveolar CD4 + CD25 + Foxp3 + T-regulatory cell ratio in acute respiratory distress syndrome is associated with increased 30-day mortality. Intensive Care Med. 2013; 39:1743–1751.
19. Nakajima T, Suarez CJ, Lin KW, Jen KY, Schnitzer JE, Makani SS, Parker N, Perkins DL, Finn PW. T cell pathways involving CTLA4 contribute to a model of acute lung injury. J Immunol. 2010; 184:5835–5841.
20. Risso K, Kumar G, Ticchioni M, Sanfiorenzo C, Dellamonica J, Guillouet-de Salvador F, Bernardin G, Marquette CH, Roger PM. Early infectious acute respiratory distress syndrome is characterized by activation and proliferation of alveolar T-cells. Eur J Clin Microbiol Infect Dis. 2015; 34:1111–1118.
21. Yu ZX, Ji MS, Yan J, Cai Y, Liu J, Yang HF, Li Y, Jin ZC, Zheng JX. The ratio of Th17/Treg cells as a risk indicator in early acute respiratory distress syndrome. Crit Care. 2015; 19:82.
22. Yan Z, Xiaoyu Z, Zhixin S, Di Q, Xinyu D, Jing X, Jing H, Wang D, Xi Z, Chunrong Z, Daoxin W. Rapamycin attenuates acute lung injury induced by LPS through inhibition of Th17 cell proliferation in mice. Sci Rep. 2016; 6:20156.
23. Manel N, Unutmaz D, Littman DR. The differentiation of human T(H)-17 cells requires transforming growth factor-beta and induction of the nuclear receptor ror-gamma. Nat Immunol. 2008; 9:641–649.
24. Fu H, Xu H, Chen H, Li Y, Li W, Zhu Q, Zhang Q, Yuan H, Liu F, Wang Q, Miao M, Shi X. Inhibition of glycogen

synthase kinase 3 ameliorates liver ischemia/reperfusion injury via an energy-dependent mitochondrial mechanism. J Hepatol. 2014; 61:816–824.

25. Wang D, Sul HS. Insulin stimulation of the fatty acid synthase promoter is mediated by the phosphatidylinositol 3-kinase pathway. involvement of protein kinase B/Akt. J Biol Chem. 1998; 273:25420–25426.
26. Chang Y, Wang J, Lu X, Thewke DP, Mason RJ. KGF induces lipogenic genes through a PI3K and JNK/SREBP-1 pathway in H292 cells. J Lipid Res. 2005; 46:2624–2635.
27. Li YH, Fu HL, Tian ML, Wang YQ, Chen W, Cai LL, Zhou XH, Yuan HB. Neuron-derived FGF10 ameliorates cerebral ischemia injury via inhibiting NF-κB-dependent neuroinflammation and activating PI3K/Akt survival signaling pathway in mice. Sci Rep. 2016; 6:19869.
28. Ma CS, Chew GY, Simpson N, Priyadarshi A, Wong M, Grimbacher B, Fulcher DA, Tangye SG, Cook MC. Deficiency of Th17 cells in hyper IgE syndrome due to mutations in stat3. J Exp Med. 2008; 205:1551–1557.
29. Renner ED, Rylaarsdam S, Anover-Sombke S, Rack AL, Reichenbach J, Carey JC, Zhu Q, Jansson AF, Barboza J, Schimke LF, Leppert MF, Getz MM, Seger RA, et al. Novel signal transducer and activator of transcription 3 (STAT3) mutations, reduced T(H)17 cell numbers, and variably defective STAT3 phosphorylation in hyper-IgE syndrome. J Allergy Clin Immunol. 2008; 122:181–187.
30. Jeffery HC, Jeffery LE, Lutz P, Corrigan M, Webb GJ, Hirschfield GM, Adams DH, Oo YH. Low-dose interleukin-2 promotes STAT-5 phosphorylation, Treg survival and CTLA-4-dependent function in autoimmune liver diseases. Clin Exp Immunol. 2017; 188:394–411.
31. Balwani S, Chaudhuri R, Nandi D, Jaisankar P, Agrawal A, Ghosh B. Regulation of NF-κB activation through a novel PI-3K-independent and PKA/Akt-dependent pathway in human umbilical vein endothelial cells. PLoS One. 2012; 7:e46528.